Microscopic and macroscopic solvation of aromatic molecules in aliphatic hydrocarbons

ARTICLE *in* CHEMICAL PHYSICS LETTERS · FEBRUARY 1991

Impact Factor: 1.9 · DOI: 10.1016/0009-2614(91)90061-D

3 AUTHORS, INCLUDING:

Uzi Even
Tel Aviv University
176 PUBLICATIONS **5,261** CITATIONS

SEE PROFILE

Joshua Jortner
Tel Aviv University
717 PUBLICATIONS **30,037** CITATIONS

SEE PROFILE

Microscopic and macroscopic solvation of aromatic molecules in aliphatic hydrocarbons

Narda Ben-Horin, Uzi Even and Joshua Jortner
School of Chemistry, Tel-Aviv University, 69978 Tel-Aviv, Israel

Received 1 September 1991; in final form 24 November 1990

The $S_0 \rightarrow S_1$ transition of heteroclusters of anthracene and tetracene with alkanes was interrogated by resonant two-colour two-photon ionization. The microscopic spectral shifts of tetracene·heptane$_n$ ($n=1$–12) clusters converge for $n>7$ to those of the tetracene–heptane solution spectra, documenting a spectroscopic manifestation of the gradual "transition" from finite to infinite systems.

1. Introduction

Recent studies of heteroclusters consisting of a large aromatic molecule (M) bound to rare-gas atoms [1–5], to small molecules [6–8], to aromatic molecules [9–12], and to aliphatic hydrocarbons [7,13–15] exhibit pronounced cluster size effects on the electronic spectrum of the "solute". Of considerable interest are microscopic solvation effects on the electronic excitations and ionization of M in the cluster, e.g., the position and the width of the electronic origin of the $S_0 \rightarrow S_1$ transition [1–15], the pure radiative lifetime of the S_1 state [16] and the ionization potential of the ground state S_0 [7,17–19]. All these cluster-size-dependent experimental observables are expected to tend towards the bulk limit with increasing cluster size. It is interesting to note that on the basis of some examples, e.g., the energetics and the radiative lifetime of electronic excitations [16], it is apparent that the functional size dependence of different observables is not universal. Nevertheless, it can be concluded that the condensed phase corresponds to an infinite cluster. Although it is often stated [20,21] that clusters provide a bridge between molecular and condensed-matter chemical physics, and this has been borne out by a multitude of theoretical results [22] the experimental implications of the gradual "transition" from a finite to an infinite system are only now emerging [23]. Spectroscopic methods provide a powerful approach for the interrogation of these novel phenomena.

In this Letter we examine the spectroscopic relations between excited-state energetic of heteroclusters and of bulk solvated molecules, reporting on the electronic spectroscopy of van der Waals heteroclusters consisting of large aromatic molecules and aliphatic hydrocarbons. We have studied the $S_0 \rightarrow S_1$ transition of heteroclusters of anthracene or tetracene with pentane, hexane and heptane in supersonic expansions. Resonant two-colour two-photon ionization in conjunction with mass-selective spectroscopy was used. This technique allows for the measurement of fragmentation-free spectra. The major questions addressed by our study are:

(1) A search for an analogy between the aromatic molecule–hydrocarbon heterocluster spectra and the spectra of the same aromatic molecule in a Shpol'skii matrix [24]. A Shpol'skii matrix constitutes a frozen normal alkane glass in which the host molecule carbon skeleton is equal to the longest dimension of the carbon skeleton of the solute aromatic molecule. In these matrices the solute–solvent electron–phonon coupling is weak, resulting in a pronounced, sharp zero-phonon line [25]. It is interesting to inquire whether such size-matching effects will be exhibited in a vdW complex.

(2) The origins of line-broadening of the spectral features of the cluster [26,27]. In the mass-resolved

0009-2614/91/$ 03.50

heterocluster spectra intrinsic inhomogeneous broadening can originate from a static distribution of isomers of the same size. Homogeneous broadening arises from large-amplitude motion, which constitute the precursors of phonons. This intermolecular motion may allow cluster reorganization at higher temperatures.

(3) Size effects on the cluster spectra and convergence to the spectrum in the condensed phase.

2. Experimental methods

Our experimental technique for resonant two-photon two-colour ionization has been described [26,27]. Briefly, the cluster beam was generated in a three-chamber differentially pumped vacuum system. The first chamber contained a magnetically actuated pulsed valve with a conical nozzle (0.5 mm diameter, 30° angle). The stagnation pressure was 1–3 atm and the valve opening time 70 μs. As a carrier gas, we used a mixture of 70% neon and 30% helium, with the expansion mixture composition containing 90% carrier gas, 5% aliphatic hydrocarbon (pentane, hexane or heptane) and 1 Torr of the aromatic molecule (anthracene or tetracene, which were heated in the nozzle to temperatures of 160 and 180°C, respectively). The beam was skimmed and passed to the chamber containing a reflectron time-of-flight mass spectrometer. The mass spectrometer, with a "Daley" ion detector for high mass sensitivity, was operated with a delayed pulsed extraction (2 μs) so that the ionization occurred in a field-free volume. A resolution of $M/\Delta M = 500$ was achieved up to masses of 2000 amu. The cluster beam was probed by a two-colour threshold ionization. An excimer laser (Lambda Physik 150 msc) was used for pumping two dye lasers (Lambda Physik). The two mildly focused (3 mm beam waist) laser beams, overlapping at the ionization volume of the mass spectrometer were aligned for counter propagation with the cluster beam, resulting in a relatively long ionization cylinder (≈ 5 mm long). The first excitation step of 1 mJ pulse energy and 0.2 mJ for the second step, with a laser pulse duration of 20 ns, were sufficient to generate 10^3 ions per pulse of the parent molecule. The laser peak power for the first pulse was 3×10^5 W cm^{-2}, so that saturation effects were small. Independent wavelength tuning of each laser allowed us to excite selectively a given cluster and ionize it at its threshold so as to minimize the excess energy leading to fragmentation. No evidence for fragmentation was found near threshold ionization (100 cm^{-1}) as inferred from (i) the appearance of distinct spectral features for each composition of a vdW complex, (ii) the absence of ionic fragments which may originate from dissociation of the van der Waals ion.

3. Results and discussions

3.1. Size-matching

In pursuing the analogy between size-matching of the solvent–solute in the Shpol'skii matrix and in the corresponding vdW clusters, we have studied the $S_0 \rightarrow S_1$ transitions of anthracene·H_1 (H ≡ pentane, hexane and heptane), which are presented in fig. 1. The electronic origin of the $S_0 \rightarrow S_1$ transition of anthracene·pentane and anthracene·hexane are narrow, being characterized by the line widths (fwhm) of 2–3 cm^{-1}, which is comparable to the width of the electronic origin of the bare anthracene molecule under similar expansion conditions (fig. 1). The line-broadening of the lowest-energy intense spectral feature of the anthracene, anthracene·pentane and anthracene·hexane originates from the (unresolved) rotational structure of the electronic origin. Weak spectral features appear on the higher-energy side of the electronic origin (fig. 1) with the frequencies (in cm^{-1}) 11, 13, 23, 24, 29, 33, 36, 41, 43, 45, 49, 58, 71, 81 for anthracene·pentane and 13, 21, 24, 34, 71, 85, 87, 94, 97 for anthracene·hexane. These weak spectral features are tentatively attributed to intermolecular hydrocarbon–aromatic molecule vibrations and also possibly low-frequency intramolecular vibrational excitations within the bound hydrocarbon.

The line-broadening of the electronic origin is different for the anthracene·heptane vdW complex, where the lowest energy spectral features exhibit a compound, broad spectral structure, with the lowest-energy spectral feature being characterized by a width (fwhm) of ≈ 20 cm^{-1}, the total width being ≈ 70 cm^{-1} (fig. 1). Our observation of the appreciable

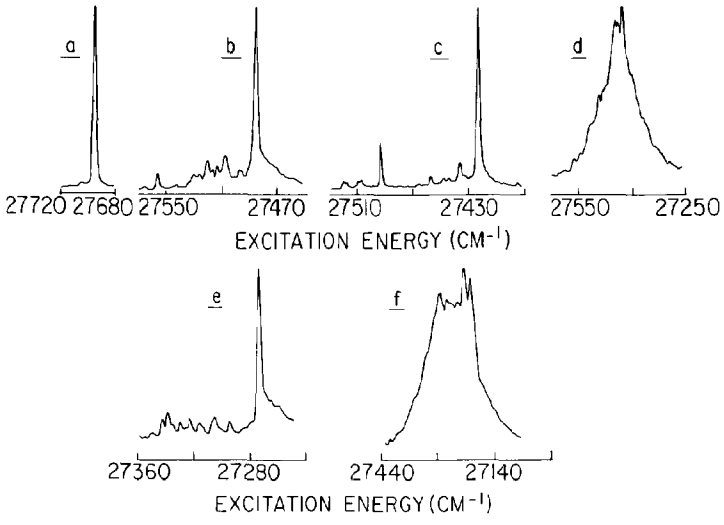

Fig. 1. Excitation spectra of mass-selected anthracene·H_n (H≡pentane, hexane, heptane) clusters in pulsed supersonic beams obtained by resonant two-photon two-colour ionization. (a) Bare anthracene, (b) anthracene·pentane, (c) anthracene·hexane, (d) anthracene·heptane, (e) anthracene·pentane$_2$, (f) anthracene·hexane$_2$.

line-broadening of the anthracene·heptane complex is qualitatively different from the results of Babbitt and Topp [15], who observed a narrow line spectrum for this system. The appreciable line-broadening (fig. 1d) is tentatively attributed to the coexistence of isomers of the anthracene·heptane complex with (i) the alkane occupying different geometrical sites on the aromatic molecule and/or (ii) the alkane exhibiting many different conformers of the anti, gauche and eclipsed type. Superimposed on such a broad isomer structure of anthracene·heptane are some sharp spectral features, which may be due to intermolecular hydrocarbon–aromatic molecule vibrations.

Spectral congestion originating from isomer structure is exhibited for some larger-size complexes of anthracene, e.g., anthracene·hexane$_2$ (fig. 1). While the anthracene·hexane$_1$ spectral structure is remarkably narrow, the anthracene·hexane$_2$ structure is smeared out. This remarkable broadening in the latter case presumably originates from two hydrocarbon molecules occupying different geometrical sites on an anthracene molecule, e.g., one-sided and two-sided structures together with the existence of structural isomers of the alkane. This compound structure of anthracene·hexane$_2$ precluded the study of higher-sized complexes of anthracene.

There is no analogy between the heterocluster aromatic molecule–hydrocarbon and the Shpol'skii matrix spectra. The size-matching between the normal alkane and the aromatic molecule in a Shpol'skii matrix is expected to be exhibited for anthracene·heptane. In contrast, the electronic origins of the $S_0 \rightarrow S_1$ transition of the non-size-matched anthracene·H (H=pentane, hexane) are narrow while that of the size-matched anthracene·heptane is smeared out due to the coexistence of isomers. Thus isomer coexistence effects preclude the analogy between small heteroclusters and the corresponding Shpol'skii matrix.

3.2. Spectral shifts and ionization potentials

The red spectral shifts $\delta\nu$ of the electronic origins of the aromatic molecule–hydrocarbon clusters of anthracene and of tetracene with pentane, heptane and hexane (table 1) are quite appreciable, being in the range -210 to -280 cm^{-1} per molecule of the aliphatic hydrocarbon. These red spectral shifts, which are considerably larger than those for rare-gas atoms, originate from dispersive interactions [2,3].

Table 1
Spectral shifts and ionization potentials (in cm^{-1})

Cluster	$\delta\nu$ [a]	Δ [a]	δI [a,b]
anthracene·pentane	−212	3	−89
anthracene·pentane$_2$	−419	3	−174
anthracene·hexane	−274	2	−161
anthracene·hexane$_2$	−486	30 [c]	-
		140 [d]	
anthracene·heptane	−267	21 [b]	-
		66 [d]	
tetracene·heptane	−252	7	−29
tetracene·heptane$_2$	−498	29	−81

[a] $\delta\nu$: spectral shift of the electronic origin (or the lowest energy spectral feature) relative to the bare molecule. Δ: fwhm of the electronic origin (or the lowest-energy spectral feature). δI: shift of the ionization potential of the complex relative to the bare molecule (obtained from linear extrapolation of the ion current).

[b] Two-photon ionization potentials (determined from thresholds) of the bare molecules are: anthracene $I = 59895$ and tetracene $I = 55966$ cm^{-1}.

[c] fwhm of the lowest-energy spectral feature.

[d] fwhm of the composite spectral feature.

The spectral shifts are approximately additive for $n=1$ and $n=2$. This additivity of the spectral shift per added alkane indicates that the $n=2$ complexes correspond to two-sided structures, with the two hydrocarbon molecules occupying opposite microsurfaces of the aromatic molecule. All these characteristics for complexes of alkanes with linear aromatic hydrocarbons are similar to those reported [7,13,14] for the complex of alkanes with the paracondensed aromatic hydrocarbon perylene.

Additional information is inferred from ionization potentials of the vdW complexes of alkanes with aromatic molecules. The ionization potentials were obtained from the two-photon onsets of the ion currents and linearly extrapolated to the ionization threshold (fig. 2). The shifts δI of these ionization potentials of the complex relative to the bare molecule (table 1) are to lower energies, being considerably smaller in their absolute magnitude than the corresponding dispersion spectral shifts. This pattern conforms with previous results of Topp and coworkers [7] for δI and $\delta\nu$ of the complexes of perylene with alkanes. The relation $|\delta\nu| \gg |\delta I|$ indicates that, while the dominating contribution to $\delta\nu$ originates from dispersive interactions which stabilize the electronically excited state, a major contribution to δI is due to intermolecular overlap interactions, which enhance repulsive interactions in the ionic state [19].

3.3. Spectroscopy of tetracene·heptane clusters

We have studied the evolution of spectral size effects in mass-selected tetracene·heptane$_n$ ($n=1$–12) clusters, whose resonant two-photon ionization spectra are portrayed in fig. 3. These spectra reveal the following characteristics:

(1) Well characterized spectral features for $n=1$–5.

(2) Appearance of the pronounced intramolecular 314 cm^{-1} vibration of the tetracene molecule in the smaller complexes, which could be well resolved for $n=1$–4.

(3) Appearance of intermolecular vibrational modes exhibited as weak spectral features (relative intensity to 0-0 is smaller than 0.2) for $n=1$–4, which are superimposed both on the origin and on the 314 cm^{-1} intramolecular vibration of the complex. These most pronounced intermolecular vibrations (in cm^{-1}) are 21, 25, 32, 48, 57, 75 and 89 for $n=1$; 29 and 89 for $n=2$; 93 for $n=3$. Such intermolecular vibrations may correspond to both tetracene·heptane relative motion and to intermolecular motion of the heptane ligand.

(4) Appearance of additional intense spectral features whose spectra are well resolved for $n=2$ and $n=6$, and which are attributed to structural isomers. The spectral shifts (relative intensity) of these most pronounced spectral features of isomers are (fig. 3) 82 cm^{-1} (0.8) for $n=2$; 45 cm^{-1} (0.9) and 205 cm^{-1} (0.9) for $n=6$. Some weaker features (45 cm^{-1} (0.2) for $n=3$; 56 cm^{-1} (0.3) for $n=4$; and 14 cm^{-1} (0.3) for $n=5$) may be due either to isomers or to intramolecular vibrations.

(5) The spectral shifts relative to the electronic origin of bare tetracene, which correspond to the lowest-energy intense spectral feature, i.e. the electronic origin of the complex (for $n=1$) or of its most abundant isomer (for $n \geq 2$), are portrayed in fig. 4. The incremented shift per added ligand $\delta(n) = \delta\nu(n) - \delta\nu(n-1)$ decreases gradually with increasing n, being $\delta(1) = -250$, $\delta(2) = -246$, $\delta(3) = -156$, $\delta(4) = -160$ and $\delta(5) = -12$ cm^{-1}, for the smaller clusters.

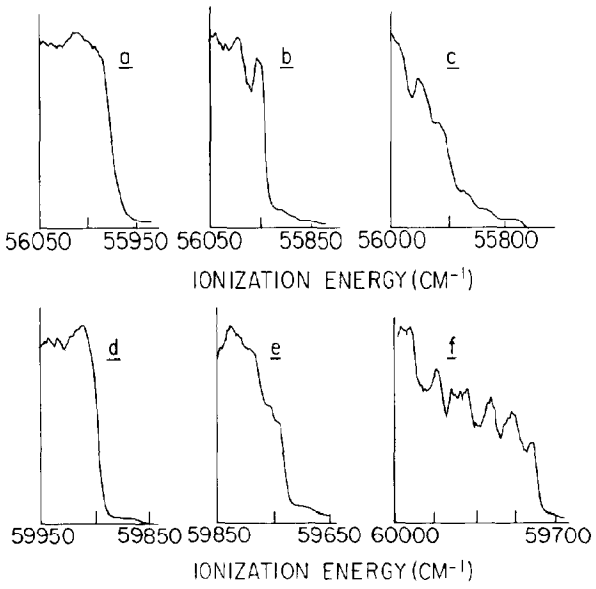

Fig. 2. Ion current spectra of mass-selected clusters of anthracene and tetracene with alkanes, obtained by resonant two-photon two-colour ionization. (a) Tetracene, (b) tetracene·heptane, (c) tetracene·heptane$_2$, (d) anthracene, (e) anthracene·pentane$_2$, (f) anthracene·hexane. The exciting laser was fixed on the $S_0 \rightarrow S_1$ origin, while the wavelength of the ionizing laser was scanned.

(6) The linewidth (fwhm) of the lowest energy spectral features of the small clusters is moderately narrow, $\Delta = 30$–$40\ cm^{-1}$ for $n = 2$–5.

(7) Structural information can be inferred for the spectral shifts (points (4) and (5)). The additivity of the spectral shifts for $n=1$ ($\delta\nu(1) = -252\ cm^{-1}$) and $n=2$ ($\delta\nu(2) = -498\ cm^{-1}$), i.e. $\delta\nu(2) \approx 2\delta\nu(1)$, indicates that the most stable $n=2$ isomer is a two-sided (1+1) structure [#1] with the two heptane molecules lying above and below the tetracene plane. The intense isomer of $n=2$ with $\delta\nu'(2) = -416\ cm^{-1}$ is attributed to the one-sided (2+0) structure. The prominent $n=3$ feature with $\delta\nu(3) = -654\ cm^{-1}$, which is close to the value of $\delta\nu(1) + \delta\nu'(2) = -668\ cm^{-1}$, is attributed to the (2+1) structure. The close proximity of the incremental spectral shifts for $n=3$ and $n=4$, i.e $\delta(3) = \delta(4) \approx -160\ cm^{-1}$, reveals that the dominating $n=4$ structure is (2+2). Thus the $n=1$–4 structures correspond to the ligands lying above and below the tetracene plane, presumably parallel to its long axis. The dramatic decrease of $\delta(5)$ relative to $\delta(4)$, suggests that the fifth heptane lies in the plane of the tetracene, resulting in the $(2+2+1_\sigma)$ structure [#1].

(8) The spectrum of the $n=6$ cluster is unique, being smeared out over a broad range of $250\ cm^{-1}$. At least three spectral features of approximately equal intensity are exhibited in the spectrum (fig. 3). The spectral shift of the lowest-energy $n=6$ feature, $\delta\nu(6) = -1057\ cm^{-1}$, is high, the incremental shift being $\delta(6) = -233\ cm^{-1}$, which is considerably larger than $\delta(5) = -12\ cm^{-1}$, while the spectral shift of the highest-energy $n=6$ spectral feature $\delta\nu'(6) = -850\ cm^{-1}$ is close to the shift $\delta\nu(5) = -825\ cm^{-1}$ of the $n=5$ cluster. The highest-energy $n=6$ spectral feature, whose incremental spectral shift $\delta\nu'(6) = \delta(6) - \delta\nu(5) = -25\ cm^{-1}$ is close to $\delta(5)$, is attributed to the addition of the sixth ligand to the first solvation layer resulting in a $(2+2+1_\sigma+1_\sigma)$ structure. The appearance of the $n=6$ cluster with a large red spectral shift $\delta(6) = -233\ cm^{-1}$ (which exceeds $\delta(5)$ and $\delta'(6)$ by one order of magnitude) is surprising, implying the appearance of a new clus-

[#1] The structure of small clusters ($n=6$) with the heptane molecules parallel to the molecular axis will be labelled by $(n_1 + n_2 + m_{1\sigma} + m_{2\sigma})$, which designates n_1 and n_2 ligands below and above the tetracene plane and m_1 and m_2 ligands located in the tetracene plane on both its sides.

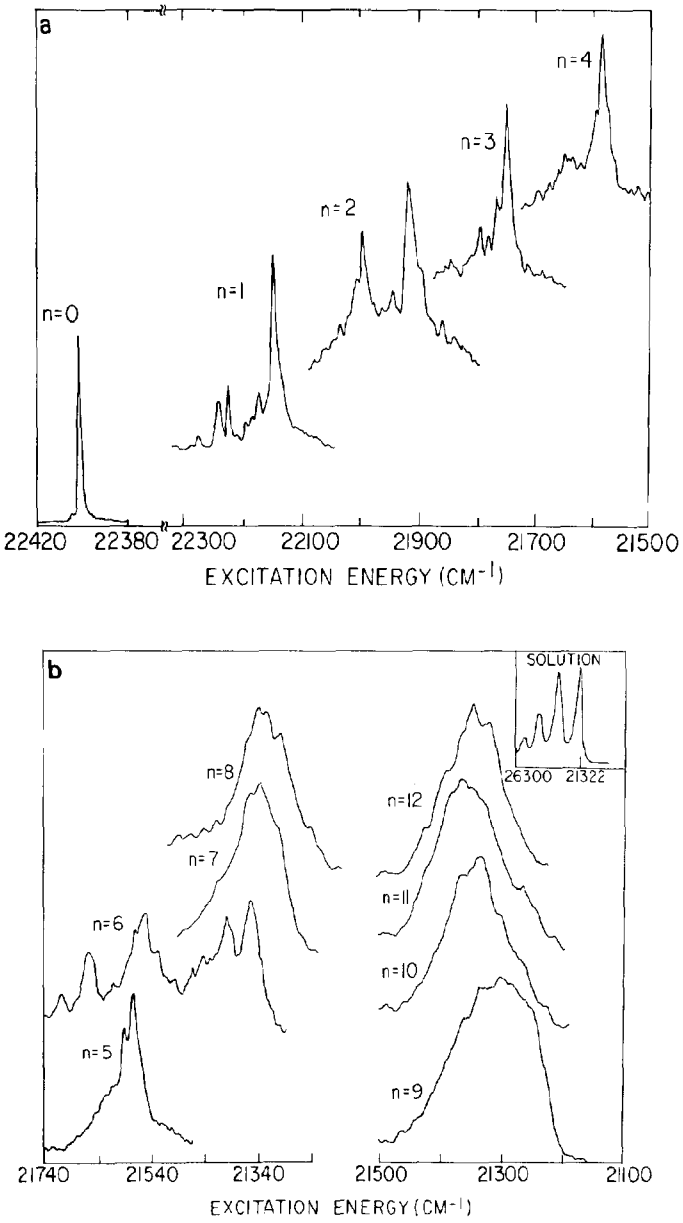

Fig. 3. Excitation spectra of mass-selected tetracene·heptane$_n$ (n=0–12) clusters obtained by resonant two-photon two-colour ionization. (a) n=1–4, while n=0 corresponds to the bare molecule. (b) n=5–12. The insert on the top (marked: solution) corresponds to the fluorescence excitation spectrum of tetracene in liquid heptane at 300 K. (The fluorescence was collected at 4700 Å.) The broad peaks are at 4690, 4400 and 4130 Å.

ter structure (marked S), which may involve a perpendicular arrangement of ligand(s) relative to the long axis of tetracene. An additional n=6 structure is manifested (fig. 3) by the appearance of a spectral shift $\delta\nu''(6) = -1012\ \mathrm{cm}^{-1}$ ($\delta''(6) = -188\ \mathrm{cm}^{-1}$). Thus the n=6 cluster marks the closure of the first solvation layer together with proliferation of structural isomers.

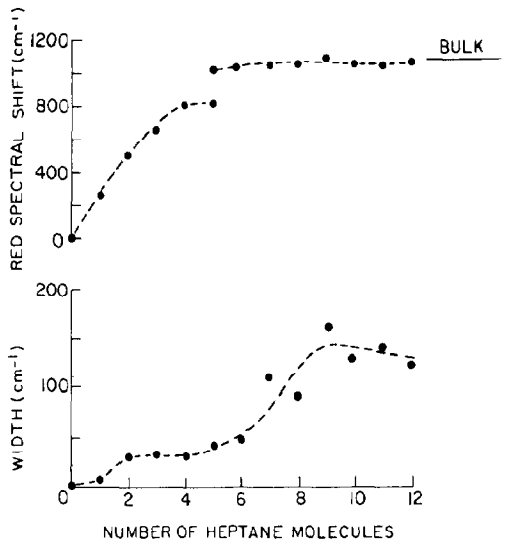

Fig. 4. Size dependence of the red spectral shift and the width of the line (fwhm) of the prominent lowest-energy spectral feature of the $S_0 \rightarrow S_1$ transition of tetracene·heptane$_n$ clusters. The dashed curves serve only to guide the eye.

(9) A qualitative change in the cluster spectra is exhibited for $n \geqslant 7$ (figs. 3 and 4) where the spectral features become broadened ($\Delta = 100$–130 cm^{-1} for $n = 7$–12) and no significant structure can be resolved. The linewidth of the large clusters reveals some fluctuations in the range $n \geqslant 7$, e.g., reaching a maximum at $n = 9$. The linewidth saturates at $n = 10$–12, reaching the value $\Delta = 120$ cm^{-1}. Such a "slush-like" broadened structure can originate either from the overlap of a large number of static isomers at relatively low temperatures or from dynamic isomerization at higher temperatures. Molecular dynamics simulations of large (aromatic molecule)·(rare gas)$_n$ ($n = 5$–30) clusters indicate that static broadening prevails for $T < 35$ K. In view of an ignorance of the temperature of the tetracene·heptane$_n$ clusters we cannot assert whether the broadening is static or dynamic.

(10) In the range $n \geqslant 7$ the total spectral shift is constant, assuming the value $\delta\nu(n) = -1080 \pm 20$ cm^{-1} for $n = 7$–12.

The first solvation layer is closed for $n = 6$, which exhibits the coexistence of several isomers, e.g., $(2+2+1_\sigma+1_\sigma)$ and S. The close proximity of the spectral shifts of the $n = 7$–12 clusters and the lowest-energy $n = 6$ cluster (the S structure), implies that the structure of the $n \geqslant 7$ clusters involves the buildup of the second solvation layer on the S structure of the first solvation layer. The spectral shift in this system is dominated by short-range attractive interactions, and is expected to nearly saturate when the first layer is closed, which is in accord with the saturation of $\delta\nu$ for $n \geqslant 6$ (fig. 4). The building of the second layer for $n \geqslant 7$ (fig. 4) results in additional line-broadening which may be due to some of the following sources: (i) enhanced static disorder in the second layer, (ii) induction of the structural changes of the ligands in the first layer by the building of the second layer, (iii) dynamic disorder in the second layer or due to exchange between the first and second layers.

It is interesting to compare these data for large tetracene·heptane$_n$ clusters with the solution spectra of tetracene in heptane (see insert in fig. 3b), which is characterized by a spectral shift of $\delta\nu \approx -1080$ cm^{-1} (relative to the electronic origin of the supersonically cooled bare molecule) and a linewidth of $\Delta \approx 440$ cm^{-1} for the lowest-energy spectral feature at 300 K. The line-broadening in solution $\Delta = 440$ cm^{-1} is considerably larger than in the large clusters $\Delta = 120$ cm^{-1} (for $n = 10$–12). The high-temperature (300 K) solution spectra result in two additional types of line-broadening which are not reflected in the low-temperature (though unknown) cluster spectra: (i) intrinsic line-broadening due to intramolecular vibrational sequence congestion effects in the large tetracene molecule, (ii) enhancement of static and dynamic isomerization effects at a higher temperature. Low-temperature spectra of tetracene in heptane glasses will be useful for further comparison of line-broadening, however, these will be complicated by site splitting effects [24,25] and will require careful preparation by thermal annealing. In contrast to the marked temperature effect on the line-broadening, the spectral shifts are expected to exhibit a moderately weak temperature dependence, allowing for the exploration of spectroscopic size effects with comparison of the cluster spectra and room-temperature solutions spectra. The spectral shift $\delta\nu = -1080 \pm 10$ cm^{-1} of the $n = 7$–12 clusters practically coincides with the spectral shift $\delta\nu = -1080$ cm^{-1} for the lowest-energy composite spectral feature of tetracene in heptane (fig. 4). The spectral shift in this system is dominated by short-range at-

tractive interactions. Accordingly, it is expected that the first solvation layer of the hydrocarbon will result in a spectral shift which is close to the bulk value. For tetracene·heptane$_n$ clusters the convergence of the cluster spectral shift to the bulk limit is accomplished for low values of $n \geq 7$, which mark the saturation of the first solvation layer in such "chemical-type" clusters. This result demonstrates the convergence of the cluster spectra to the spectrum of the condensed phase, bridging the gap between the excited-state energetics of finite and infinite systems of chemical interest.

Acknowledgement

This research was supported by the Basic Research Fund administered by the Israel Academy of Sciences (to UE), by the German–Israel Binational Science Foundation (to UE) and by the James Franck programme at Tel-Aviv University.

References

[1] A. Amirav, U. Even and J. Jortner, J. Chem. Phys. 75 (1981) 2489.
[2] U. Even, A. Amirav, S. Leutwyler, M.J. Ondrechen, Z. Berkovitch-Yellin and J. Jortner, Discussions Faraday Soc. 73 (1982) 153.
[3] S. Leutwyler and J. Jortner, J. Phys. Chem. 91 (1987) 5558.
[4] S. Leutwyler and J. Bösiger, in: Large finite systems, eds. J. Jortner and B. Pullman (Reidel, Dordrecht, 1987) p. 153.
[5] M.M. Doxtader, I.M. Gulis, S.A. Schwartz and M.R. Topp, Chem. Phys. Letters 112 (1984) 483.
[6] U. Even and J. Jortner, J. Chem. Phys. 78 (1983) 3445.
[7] M.I. Shckuka, A.L. Motyka and M.R. Topp, Chem. Phys. Letters 164 (1989) 87.
[8] S.A. Wittmeyer and M.R. Topp, Chem. Phys. Letters 163 (1989) 261.
[9] M.M. Doxtader and M.R. Topp, Chem. Phys. Letters 124 (1986) 39.
[10] M.M. Doxtader, E.A. Mangle, A.K. Bhattacharya, S.M. Cohen and M.R. Topp, Chem. Phys. 101 (1986) 413.
[11] R.J. Babbitt and M.R. Topp, Chem. Phys. Letters 127 (1986) 111.
[12] D.C. Easter, M.S. El-Shall, M.Y. Hahn and R.L. Whetten, Chem. Phys. Letters 157 (1989) 277.
[13] M.M. Doxtader and M.R. Topp, J. Phys. Chem. 89 (1985) 4291.
[14] E.A. Mangle and M.R. Topp, Chem. Phys. 112 (1987) 427.
[15] R.J. Babbitt and M.R. Topp, Chem. Phys. Letters 135 (1987) 182.
[16] A. Penner, A. Amirav, J. Jortner, A. Nitzan and J. Gersten, J. Chem. Phys. 93 (1990) 147.
[17] K.M. Fung, W.E. Henke, H.L. Selzle and E.W. Schlag, J. Phys. Chem. 85 (1981) 3560.
[18] J. Hager, M. Ivanco, M.A. Smith and S.C. Wallace, Chem. Phys. Letters 113 (1985) 503.
[19] N. Ben-Horin, U. Even and J. Jortner, J. Chem. Phys. 91 (1989) 331.
[20] J. Jortner, Ber. Bunsenges. Physik. Chem. 88 (1984) 188.
[21] G. Benedek, T.P. Martin and G. Pacchioni, Elemental and molecular clusters (Springer, Berlin, 1988).
[22] J. Jortner, D. Scharf, U. Landman, N. Ben-Horin and U. Even, International School of Physics Enrico Fermi (CVII Course) (North-Holland, Amsterdam, 1990), in press.
[23] C. Crépin and A. Tramer, Chem. Phys. Letters 170 (1990) 446.
[24] E.V. Shpol'skii, Soviet Phys. Usp. 6 (1963) 411; 5 (1962) 522; 3 (1961) 372.
[25] K.K. Rebane, Impurity spectra of solids (Plenum Press, New York, 1970).
[26] U. Even, N. Ben-Horin and J. Jortner, Chem. Phys. Letters 156 (1989) 139.
[27] U. Even, N. Ben-Horin and J. Jortner, Phys. Rev. Letters 62 (1989) 140.